Investigation of the biofouling properties of several algae on different textured chemical modified silicone surfaces

Jihai Xu [a,b], Wenjie Zhao [a,*], Shusen Peng [a], Zhixiang Zeng [a], Xin Zhang [a], Xuedong Wu [a,*], Qunji Xue [a]

[a] *Key Laboratory of Marine Materials and Related Technologies, Zhejiang Key Laboratory of Marine Materials and Protective Technologies, Ningbo Institute of Materials Technology and Engineering, Chinese Academy of Sciences, Ningbo 315201, China*
[b] *University of Chinese Academy of Sciences, Beijing 100049, China*

Keywords:
Biofouling
Texture
Wettability
Size
Algae

A B S T R A C T

Engineered pillars, pits and grooves spaced 3, 6, 9 and 12 μm apart were fabricated on siloxane modified acrylic resin films. The effect of feature size, geometry, and wettability on the settlement of different algae was evaluated. These films showed various antifouling performances to *Ulothrix*, *Closterium* and *Navicula*. For *Navicula* (length: 10–12 μm), the feature size and geometry displayed a substantial correlation with the antifouling properties. The film with pillars spaced 3 μm reduced *Navicula* settlement by 73% compared to the control surface. For *Closterium* (length: 45–55 μm), their responses were governed by the same underlying thermodynamic principles as wettability, the largest reduction in *Closterium*, 81%, was obtained on the surface with grooves spaced 12 μm apart. For *Ulothrix* (length: 5–8 mm), the surface also showed the best antifouling performance, the reduction ratio of the settlement on the surface with grooves spaced 12 μm apart could even reach 92%. At last, physical fouling deterrent mechanisms for the films with various textures were analyzed in detail. The feature size and geometry display a substantial correlation with the antifouling properties when the size of fouling algae is close to the textures. With the increasing size for algae, antifouling performance was getting better on surface with pillars or grooves because the algae are bridged between two or more features other than stabilizing its entire mass on one single feature or able to settle between features.

1. Introduction

Biofouling is generally defined as the accumulation of living organisms including microorganisms, algae and animals on a surface immersed in seawater. This undesirable colonization has serious impacts that can be environmental, economic, or ecological-related [1–3]. Biofouling is of great concern in numerous applications ranging from biosensors to industrial and marine equipment. The self-polishing coatings are effective on reducing biofouling because of slow release of tin, copper or other toxins in time [4–6]. But they had detrimental impact on nature [7–9]. In order to protect our nature, the development of non-toxic and environment-friendly anti-fouling paints is the main trend of marine antifouling coatings. The ideal coating should be also with antifouling and foul releasing properties.

Poly(dimethysiloxane) (PDMS) or silicone materials have demonstrated good fouling-release (FR) performance under suitable hydrodynamic conditions, and they are considered non-toxic marine coatings [10–13]. But, PDMS has some obvious drawbacks, such as poor adhesion with substrate, low mechanical strength and high cost. The siloxane modified acrylic resin (SMAR), also has good fouling-release (FR) performance, and its mechanical properties are better than silicone [14]. But, the SMAR is not inherently antifouling like other low surface energy antifouling paints. Biofouling will occur under low flow conditions.

Shark, mollusk shells and other marine animals show excellent antifouling performance on their skins because their surfaces display special micro/nano binary textures. Inspired by the interesting phenomena, the materials with micro/nano-textures on the surface might also demonstrate the excellent anti-fouling performance. Carman et al. presented a biomimetically inspired surface topography (Sharklet AFTM), which had feature dimensions smaller than the spore body, significantly reduced settlement density by 86% relative to smooth PDMS [15]. And they suggested that spores' responses were governed by the same underlying thermodynamic

* Corresponding authors. Tel.: +86 0574 86685036.
E-mail addresses: zhaowj@nimte.ac.cn (W. Zhao), xdwu@nimte.ac.cn (X. Wu).

principles as wettability. Results from Schumacher indicated that engineered microtopographies reduced *Ulva* spores settlement by up to 58% (diameter circular pillars and 10 μm equilateral triangles) and by 77% for microtopographies replicating shark skin [16]. An indirect correlation between spore settlement and a newly described engineered roughness index was identified in this research.

Previous results evaluated the effect of topographic feature size, geometry, wettability and roughness on settlement of *Ulva* zoospores, but it was necessary to address algae size in relation of attachment. All of these factors were important for the anti-fouling properties. Static bioassays were conducted on microtextured polyimide surfaces using four diatom species, *Fallaciacarpentariae*, *Nitzschia cf. paleacea*, *Amphora* sp. and *Navicula jeffreyi* with cell sizes ranging from 1–14 μm. Their work directly tested attachment 'point theory' and preliminarily revealed the effect of cell sizes on anti-fouling properties [17]. To the best of our knowledge, the relationship between algae size and texture geometry have not been reported in detail until now.

In this paper, taking advantage of low surface energy and surface textures, SMAR films with various textures are prepared. Three kinds of common algae including *Ulothrix*, *Closterium* and *Navicula* are used to evaluate the biofouling resistance properties of as-prepared samples. Systematic investigation of surface topography, wet/dewettability, anti-fouling performances are performed by corresponding equipments. The anti-fouling mechanisms of textured coatings are analyzed based on the three key factors including of surface wettability, morphology (feature size and spacing), and algae size.

2. Experimental

2.1. Materials

The polydimethylsiloxane (PDMS) elastomer (SILASTIC DC-184, Dow Corning Corporation) was used as the masterplate material for texture formation due to its high reproducibility and good elasticity. The elastomer was prepared by hand mixing ten parts by weight of PDMS prepolymer with one part by weight of curing agent. The mixture was degassed at ambient temperature for 90 min, then typically cured at 70 °C for 12 h.

The base material for topographical modification used in this study was siloxane modified acrylic resin (SMAR) (SKD002, Shanghai Chaoyu Corporation). Six parts of SMAR and two parts of hexamethylene diisocyanate trimer (CORONATE HX, NPU Corporation) were dissolved in three parts of xylene by weight. The mixture was degassed for 30 min and allowed to be cured at 70 °C for 12 h.

2.2. Surfaces

The method used to fabricate various surface textures is simple and reproducible. The schematic process flow to create pillars, pits and groove with different area density was shown in Fig. 1. The texture was initially etched in silicon wafers using the inductively coupled plasma etching process as previously described by McAuley [18]. The above PDMS mixture was degassed at room temperature for about 1.5 h to remove any air bubbles in the mixture. The PDMS mixture was spin-coated on the wafers, then heat treated at 70 °C for 12 h in a vacuum oven. Negative texture was replicated directly from the etched wafer. The PDMS elastomer with negative texture was used to produce a positive replica in SMAR. At last, the above SMAR mixture was degassed at room temperature for about 0.5 h to remove bubbles. The SMAR mixture was spin-coated on the textured PDMS elastomer, after being heat treated at 70 °C for 12 h, the positive textures were transferred to SMAR from the negative textures.

Surface textures included circular pillars, continuous grooves, and circular pits. Their diameter or width was 3 μm. Pillars, pits and grooves were spaced 3, 6, 9 and 12 μm apart (Fig. 2). Control surfaces were uniformly smooth.

2.3. Contact angle measurements

The static water contact angles of the free-standing SMAR films with textures were measured according to the sessile droplet method using a drop shape analysis system (Data Physics OCA20, Germany) with a computer-controlled liquid dispensing system. Deionized water droplet with a volume of 4 μL was employed as the source for the measurements. The contact angle was the average of three replicates for each textured sample, and each sample's contact angle was tested three times.

2.4. Algae settlement assay

SMAR samples containing 3 μm diameter circular pillars, pits and 3 μm width continuous grooves, spaced 3, 6, 9 and 12 μm apart were evaluated for settlement of algae. Three replicates of each textured type were tested as films pasted on glass slides (size: 76 mm × 25 mm). A uniformly smooth SMAR film was used in the assay and served as a control for direct comparison.

The three algae species used, *Ulothrix*, *Closterium* and *Navicula* were all harvested from the East China Sea. The length of *Ulothrix*, *Closterium* and *Navicula* was, in order, 5–8 mm, 45–55 μm and 10–12 μm, respectively; the width of three algae species was all 3–4 μm. Growth conditions for all algae were 12:12 h light:dark cycle at 25 °C. *Closterium* and *Navicula* were supplemented with Guillard's F/2 medium, *Ulothrix* was supplemented with Selenite Enrichment (SE) medium.

The glass slides with films were placed on sample holder which was immersed in the bottom of the beaker filled with 15 mL filtered seawater and 15 mL of algae culture suspension. The density of the *Closterium* and *Navicula* culture suspension was $1–3 \times 10^6$ cells mL^{-1}. The chlorophyll value of *Ulothrix* culture suspension was 1.5547 ($\mu g\,cm^{-2}$).

Then, the algae were left to be settled for 7 days. The films after algae settlement were rinsed by dipping in a new beaker of filtered seawater three times to remove unattached algae.

The films settled by *Closterium* and *Navicula* were fixed with 2% glutaraldehyde in artificial seawater as described by Callow [19]. *Closterium* and *Navicula* counts were quantified using a Dimension 3100v Laser Scanning Confocal Microscope (LSCM) analysis system. Ten images and counts were obtained from 10 random fields of view per 0.64 mm^2 area for *Closterium* and 0.16 mm^2 area for *Navicula*. The settlement of *Ulothrix* on the films was determined by chlorophyll values by using a Lambda 950 UV/Vis/NIR Spectrophotometer.

Every textured film's antifouling property was evaluated by the reduction ratio (R_r) of algae density compared to the control film.

$$R_r = \frac{(D_c - D_n)}{D_c} \quad (1)$$

D_n, the algae density of the textured film; D_c, the algae density of the control film; when the algae density of textured film was higher than control surface, the R_r then was a negative value.

3. Results and discussion

Understanding the role of surface textures in deterring different organisms is important in terms of optimizing the performance of coatings designed to prevent or reduce biofouling. The SMAR

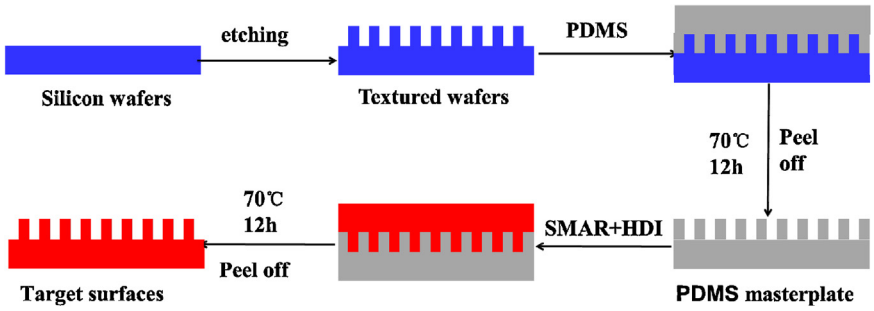

Fig. 1. Schematic process flow of the replication procedure for fabricating textured surfaces.

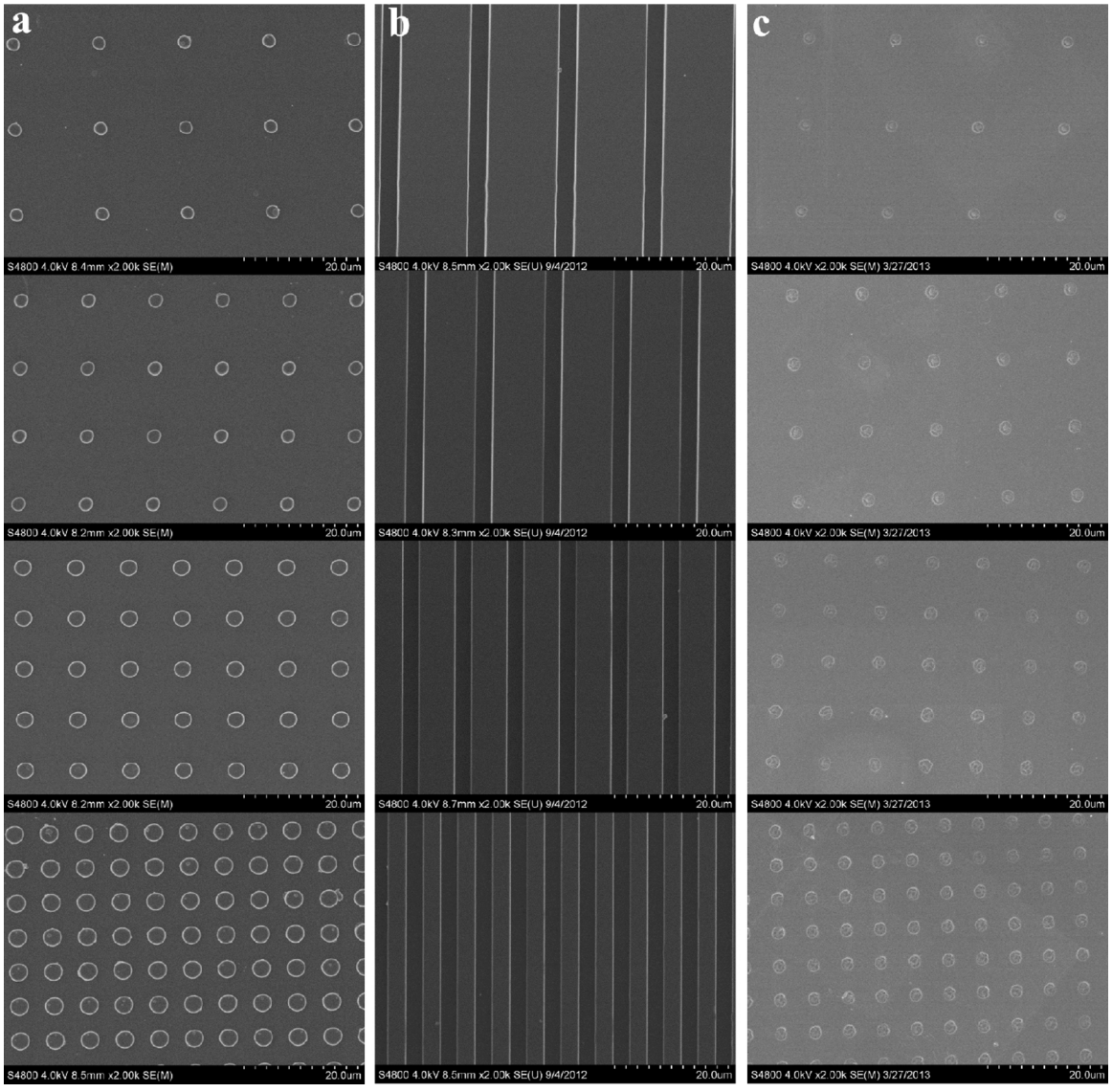

Fig. 2. SEM images of engineered textures on the SMAR surface. (a) 3 μm Diameter circular pillars spaced 12, 9, 6 and 3 μm apart; (b) 3 μm wide continuous groove, spaced 12, 9, 6 and 3 μm apart; (c) 3 μm diameter circular pits spaced 12, 9, 6 and 3 μm apart.

base material was chosen due to its excellent mechanical properties compared to fouling-release coatings. The regular pillars, pits and grooves were chosen as models in order to reveal the deep mechanism that can be used to inform further designs aimed at reducing biofouling. Three algae, *Ulothrix*, *Closterium* and *Navicula*, which were different in size, were used to reveal the relationship between algae size and texture geometry in detail.

Every textured film's antifouling property was evaluated by the reduction ratio of the settlement compared to the control film.

The *Navicula* used in this study were able to settle, glide and attach to surface in static bioassays. The size of *Navicula* was 10–12 μm, which was similar to that of textures. For the surfaces with pillars, the lowest mean *Navicula* density was found on the surface with a distance of 3 μm between adjacent pillars. This surface

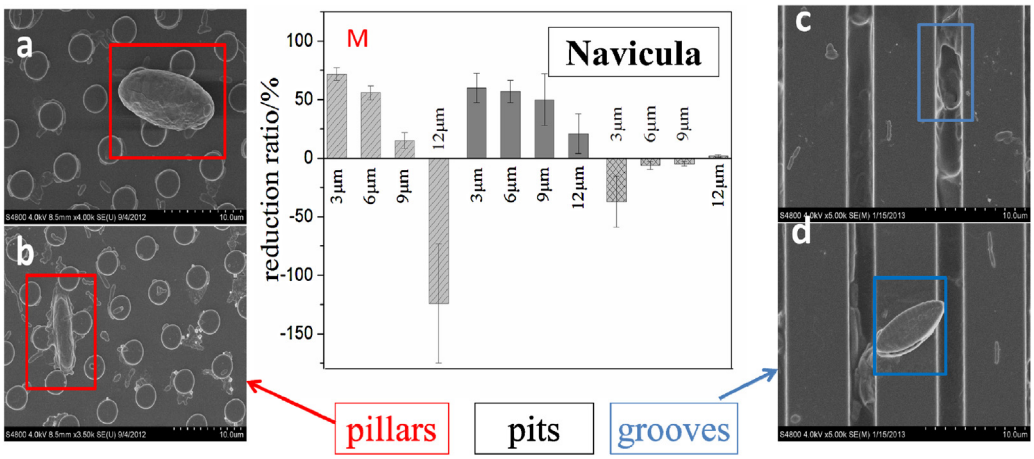

Fig. 3. *Navicula* settled on the textured surfaces. M: reduction ratio compared to the control surface; a–d: SEM images of *Navicula* settled on the surface with pillars and grooves.

showed a significant reduction ratio which was 73% compared to the control surface. As the distance of pillars increased, the reduction rate tended to be reduced. When the distance of the pillars was 12 μm, *Navicula* settlement was even more serious, which was 2.25 times than that of the control surface. For the surfaces with pits spaced 3, 6, 9 and 12 μm apart, the settlement was all lower than control surface. And with the decrease of distance between adjacent pits, the settlement reduction rate compared to the control surface tends to be increased. When the distance of the pits was 3 μm, the reduction ratio could even reach 60%.The settlement on the surface with groove spaced 12 μm apart did not change significantly compared to control surface. And higher numbers of *Navicula* attached to the surface with groove spaced 3, 6 and 9 μm apart compared to control surface (Fig. 3a).

On the surface with pillars spaced 3 μm, the *Navicula* (the length is 10–12 μm) was too large to rest between or on top of the pillars, most of them must bridge (Fig. 3a). Bridging which reduced the contact area between the *Navicula* and surface, would reduce the overall adhesion strength. So the lowest mean *Navicula* density was displayed on the pillars surface with a distance of 3 μm between adjacent pillars. With the distance of pillars increased, the probability of *Navicula* settling on the area (Fig. 3b) between the pillars tended to be increased. When the distance of pillars was 12 μm, the area between adjacent pillars was 12 μm × 12 μm, the size of the *Navicula* body are ideally suited to settlement on the scale of micrometers. So the number of *Navicula* was the maximum on the textured surface with the largest distance between adjacent pillars (2.25 times that of the control surface).

For the surfaces with pits, the diameter size of pits was 3 μm circular. When *Navicula* attached on the pits, it was too small to fit the *Navicula* entire mass and some parts of body without being in physical contact with the surface. This case would also reduce the overall adhesion area and strength. So for the surfaces with pits, the settlement were all lower than control surface, and the settlement reduction rate compared to the control surface tends to increase as the distance of pits decreases.

On the surface with grooves, a higher number of spores consistently attached to the surface with valleys than on controls and a majority of spores settled on the angle between the valley floor and sidewall. Swimming spores possessed the ability of sensing an energetically favorable place for settlement has been noted previously [20]. And recent research [21] indicated that spores of *Ulva* settled preferentially in 5 μm valleys, the same size as the spores. In this study, the width of continuous groove was 3 μm, similar to the width of *Navicula* (3–4 μm). The groove can provide a suitable place for *Navicula* settling. By observing *Navicula*'s attachment to

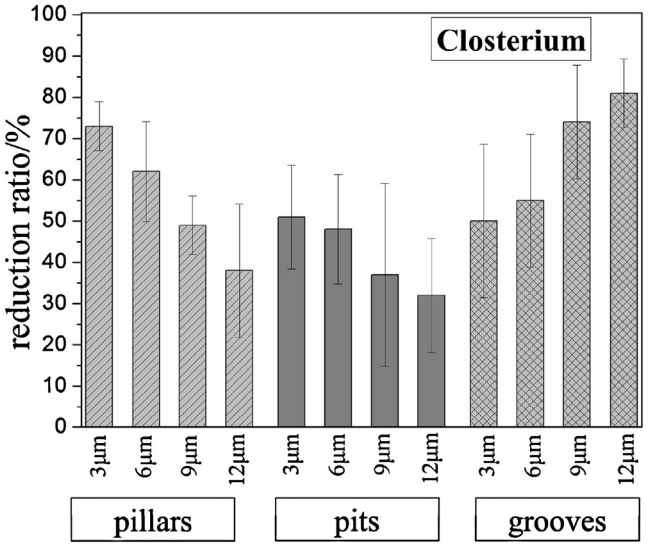

Fig. 4. *Closterium* reduction ratio of textured surfaces compared to the control surface.

the surfaces with grooves, it was found that most of *Navicula* lined up longitudinally inside the grooves (Fig. 3c), and their entire mass was glued to groove floor and sidewall which making the Navicula contact closely with surfaces, only few *Navicula* settled on the flat area (Fig. 3d). So the *Navicula* density on surface was determined by the settlement in the grooves. The surface with grooves spaced 3 μm showed the highest *Navicula* density compared to all other surface with grooves because which having the highest number of grooves. The results proved *Navicula's* settling selectivity more directly, *Navicula* settled preferentially in valleys and against pillars and pits.

Another kind of algae, *Closterium*, was used to test the antifouling performance of the textured surfaces (Fig. 4). *Closterium's* size was 45–55 μm which was much larger than that of textures. The reduction rate of the surfaces with pillars and pits both tended to be greater, as the distance of pillars or pits decreased. Compared to the control surface, the highest reduction ratio of surfaces with pillar was 73%, greater than that of surfaces with pits (51%). Relative to the control surface, the surfaces with groove spaced 3, 6, 9 and 12 μm apart all showed statistically significant reduction in *Closterium* density which distinctly different from *Navicula*. The reduction ratio of the surface with groove spaced 3 μm and 6 μm was 50% and 55%. A higher reduction ratio (74%) was obtained

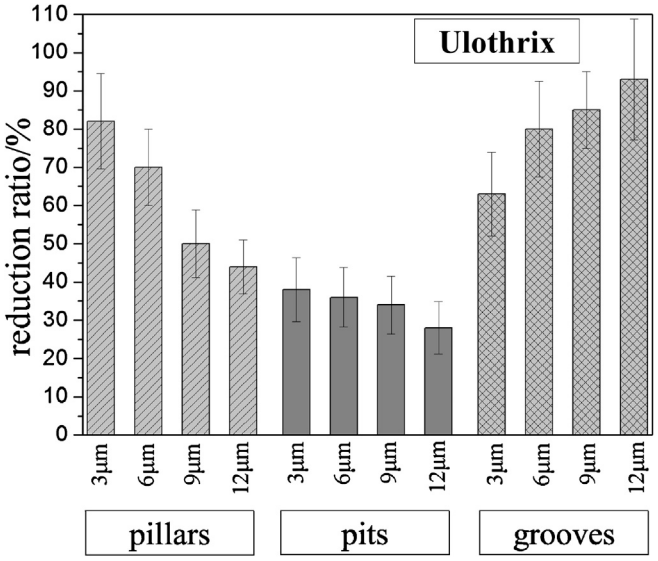

Fig. 5. *Ulothrix* reduction ratio of textured surfaces compared to the control surface.

on the surface with grooves spaced 9 μm compared to both the grooves spaced with 3 μm and 6 μm. The surface with grooves spaced 12 μm showed the highest reduction ratio (81%) compared to all other surface with grooves.

The surface with pillars, pits and grooves all showed well capability of antifouling when resisting *Closterium* which is significantly different to that of *Navicula*. Researchers presented that topography altered wettability [22,23] and wettability influenced bioadhesion [24]. Results previously confirmed that the organism's responses were governed by the same underlying thermodynamic principles as wettability when its size was much bigger than feature size [15]. *Closterium* (length: 45–55 μm) was too large to rest between or in the three textures, it should bridge on two or more pillars, pits or grooves. Considering *Closterium* settling on a textured surface, bridging is similar to the air pocket state described by the Cassie–Baxter relation or alternatively, conforming similar to Wenzel behaviour. Compared to the reduction ratio of each textured surface (Table 1), it could almost find a basic rule that a higher mean reduction ratio was obtained on a surface which had a greater contact angle of water.

In order to reveal the relationship between algae size and texture geometry in detail, we further characterized the antifouling behavior of surfaces with pillars and grooves by evaluating their inhibitory effect on the *Ulothrix* (Fig. 5). *Ulothrix's* size was 5–8 mm which was the biggest among the three algae selected.

The results of *Ulothrix*, *Closterium* and *Navicula's* reduction ratio of the surfaces with pillars showed that the surface showed markedly different antifouling performance for different algae (Fig. 6a). For the same surface, it displayed the best antifouling performance to the *Ulothrix* with the largest size. And when resisted the smallest *Navicula*, the performance became worst. For example, the reduction ratio of *Ulothrix's* settlement on the surface with pillars spaced 6 μm was 70%, for *Closterium* and *Navicula*, the reduction ratios were 62% and 56%, respectively. Anyhow, the surface with pillars spaced 3 μm always showed the highest reduction ratio, no matter resisting *Ulothrix*, *Closterium* or *Navicula*.

The surfaces with grooves displayed the similar performance (Fig. 6b). For the same surface, the best antifouling performance appeared on controlling *Ulothrix's* settling. And antifouling performance was getting worse with the decreased size of algae. For example, the reduction ratio of *Ulothrix* and *Closterium*'s

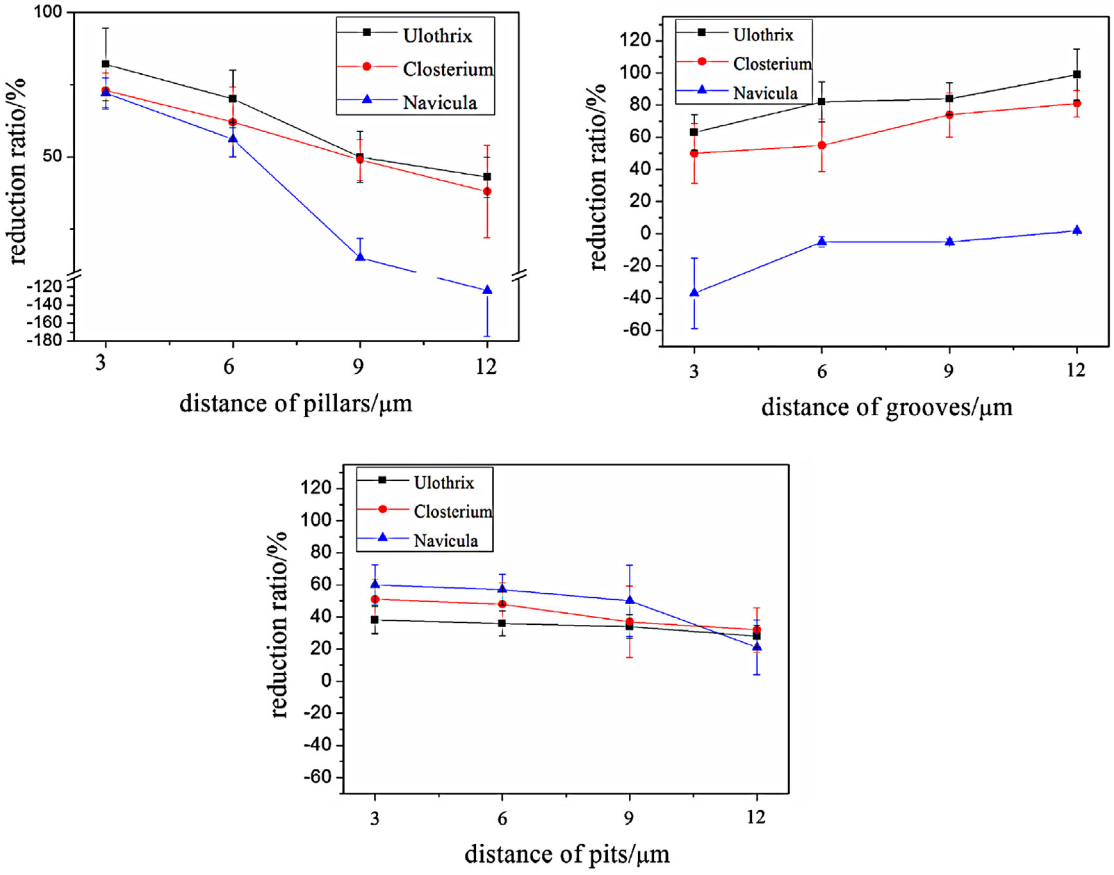

Fig. 6. The antifouling performance of surface with pillars, grooves and pits for different algae.

Table 1
The correlation between reduction ratio and surface wettability.

Surfaces	Contact angle of water (°)	Reduction ratio of *Closterium* (%)
Pit12 (spaced 12 μm)	79.5 ± 4.1	32 ± 14
Pillar12 (spaced 12 μm)	80.8 ± 1.2	38 ± 16
Pit9 (spaced 9 μm)	83.1 ± 0.1	37 ± 22
Groove3 (spaced 3 μm)	83.5 ± 2.3	50 ± 18
Pillar9 (spaced 9 μm)	85.5 ± 2.0	49 ± 7
Pit6 (spaced 6 μm)	85.7 ± 1.9	48 ± 13
Pit3 (spaced 3 μm)	87.9 ± 1.2	51 ± 12
Groove6 (spaced 6 μm)	90.9 ± 5.7	55 ± 16
Pillars6(spaced 6 μm)	92.8 ± 0.8	62 ± 12
Groove9 (spaced 9 μm)	95.1 ± 7.1	74 ± 14
Pillars3 (spaced 3 μm)	99.3 ± 0.9	73 ± 6
Groove12 (spaced 12 μm)	116.6 ± 3.7	81 ± 8

settlement of the surface with grooves spaced 3 μm could reach 63% and 50%. But, this surface settled 37% more *Navicula* than on the control surface.

For the surface with pits, the settlement reduction rate of *Ulothrix* compared to the control surface tended to increase as the distance of pits decreased like that of *Closterium* and *Navicula* because more pits reduced the adhesion area and adhesion strength. But there were no differences in the reduction rate of three algae because most body of the *Ulothrix, Closterium* or *Navicula* could contact to the flat areas of the surface with pits (Fig. 6c).

So the anti-fouling performance of textured surface was not only closely related to feature geometry and size, but also related to the algae's size. On one side, if the algae were bridged between two or more features, the attachment area and the overall adhesion strength must be reduced so that biological fouling could be deterred. But, the algae was also able to stabilize its entire mass on one single feature or be able to settle between features, they would attach more and more to the surface. When the size of fouling algae was close to the textures, the feature size and geometry displayed a substantial correlation with the antifouling properties because they determined which two settling case mentioned above the organism will select. And when the size of fouling algae was much bigger than that of the textures, the fouling organism was more likely to bridge on top of two or more features; their responses were governed by the same underlying thermodynamic principles as wettability. And antifouling performance was getting better with the bigger size of algae because the algae were more and more impossible to stabilize their entire mass on one single feature or to settle between features.

4. Conclusions

This research designed SMAR surface with regular pillars, pits and grooves. The effect of feature size, geometry, and wettability on the settlement of different algae has been thoroughly studied by comparing the antifouling performance of different surface against *Ulothrix*, *Closterium* and *Navicula*. The results predict that a textured surface which having fit feature so that the algae can bridge on between two or more features, and do not provide the area for algae displaying excellent anti-fouling performance. Synergy of both structure and surface composition provides a promising way of designing environment-benign marine anti-fouling coatings.

Acknowledgments

Financial support for this work was provided in part by National Key Basic Research Program of China (973) (2014CB643305), the National Natural Science Foundation of China (51202263 and 51335010), the China Postdoctoral Science Foundation Funded Project (2012T50564) and the Ningbo Municipal Innovation Team (2011B81001)

References

[1] R.F. Piola, K.A. Dafforn, E.L. Johnston, The influence of antifouling practices on marine invasions, Biofouling 25 (7) (2009) 633–644.
[2] M. Salta, J.A. Wharton, P. Stoodley, S.P. Dennington, L.R. Goodes, S. Werwinski, U. Mart, R.J. Wood, K.R. Stokes, Designing biomimetic antifouling surfaces, Philos. Trans. R. Soc., A: Math. Phys. Eng. Sci. 368 (1929) (2010) 4729–4754.
[3] C. Paetzold, J. Hill, J. Davidson, Efficacy of high-pressure seawater spray against colonial tunicate fouling in mussel aquaculture: inter-annual variation, Aquat. Invasions 7 (4) (2012) 555–566.
[4] J. Warnken, R.J. Dunn, P.R. Teasdale, Investigation of recreational boats as a source of copper at anchorage sites using time-integrated diffusive gradients in thin film and sediment measurements, Mar. Pollut. Bull. 49 (9-10) (2004) 833–843.
[5] A.A. Al-Juhni, B-mZ. Newby, Incorporation of benzoic acid and sodium benzoate into silicone coatings and subsequent leaching of the compound from the incorporated coatings, Prog. Org. Coat. 56 (2-3) (2006) 135–145.
[6] P. Buskens, M. Wouters, C. Rentrop, Z. Vroon, A brief review of environmentally benign antifouling and foul-release coatings for marine applications, J. Coat. Technol. Res. 10 (1) (2012) 29–36.
[7] J. Strand, J.A. Jacobsen, Accumulation and trophic transfer of organotins in a marine food web from the Danish coastal waters, Sci. Total Environ. 350 (1-3) (2005) 72–85.
[8] P.A. Turley, R.J. Fenn, J.C. Ritter, M.E. Callow, Pyrithiones as antifoulants: environmental fate and loss of toxicity, Biofouling 21 (1) (2005) 31–40.
[9] A.A. Finnie, Improved estimates of environmental copper release rates from antifouling products, Biofouling 22 (5-6) (2006) 279–291.
[10] M.K. Chaudhury, J.A. Finlay, J.Y. Chung, M.E. Callow, J.A. Callow, The influence of elastic modulus and thickness on the release of the soft-fouling green alga *Ulva linza* (syn. Enteromorpha linza) from poly(dimethylsiloxane) (PDMS) model networks, Biofouling 21 (1) (2005) 41–48.
[11] D.E. Wendt, G.L. Kowalke, J. Kim, I.L. Singer, Factors that influence elastomeric coating performance: the effect of coating thickness on basal plate morphology, growth and critical removal stress of the barnacle *Balanus amphitrite*, Biofouling 22 (1–2) (2006) 1–9.
[12] E.R. Holm, C.J. Kavanagh, A.E. Meyer, D. Wiebe, B.T. Nedved, D. Wendt, C.M. Smith, M.G. Hadfield, G. Swain, C.D. Wood, et al., Interspecific variation in patterns of adhesion of marine fouling to silicone surfaces, Biofouling 22 (3-4) (2006) 233–243.
[13] Y. Liu, C. Leng, B. Chisholm, S. Stafslien, P. Majumdar, Z. Chen, Surface structures of PDMS incorporated with quaternary ammonium salts designed for antibiofouling and fouling release applications, Langmuir 29 (9) (2013) 2897–2905 (the ACS journal of surfaces and colloids).
[14] H.J. Naghash, S. Mallakpour, N. Kayhan, Synthesis and characterization of silicone modified acrylic resin and its uses in the emulsion paints, Iran, Polym. J. 14 (3) (2005) 211–222.
[15] M.L. Carman, T.G. Estes, A.W. Feinberg, J.F. Schumacher, W. Wilkerson, L.H. Wilson, M.E. Callow, J.A. Callow, A.B. Brennan, Engineered antifouling microtopographies—correlating wettability with cell attachment, Biofouling 22 (1-2) (2006) 11–21.
[16] J.F. Schumacher, M.L. Carman, T.G. Estes, A.W. Feinberg, L.H. Wilson, M.E. Callow, J.A. Callow, J.A. Finlay, A.B. Brennan, Engineered antifouling microtopographies—effect of feature size, geometry, and roughness on settlement of zoospores of the green alga *Ulva*, Biofouling 23 (1) (2007) 55–62.
[17] A.J. Scardino, E. Harvey, R. De Nys, Testing attachment point theory: diatom attachment on microtextured polyimide biomimics, Biofouling 22 (1-2) (2006) 55–60.
[18] S.A. McAuley, H. Ashraf, L. Atabo, Silicon micromachining using a high-density plasma source, J. Phys. D: Appl. Phys. 34 (2001) 2769–2774.
[19] M.E. Callow, J.A. Callow, J. Pickett-Heaps, R. Wetherbee, Primary adhesion of *Enteromorpha* (Chlorophyta, Ulvales) propagules: quantitative settlement studies and video microscopy, J. Phycol. 33 (1997) 938–974.
[20] M.E. Callow, J.A. Callow, L.K. Ista, S.E. Coleman, A.C. Nolasco, G.P. Lopez, Use of self-assembled monolayers of different wettabilities to study surface selection and primary adhesion processes of green algal (Enteromorpha) zoospores, Appl. Environ. Microbiol. 66 (2000) 3249–3254.
[21] M.E. Callow, A.R. Jennings, A.B. Brennan, C.A. Seegert, L. Wilson, A. Feinberg, R. Baney, J.A. Callow, Microtopographic cues for settlement of zoospores of the green fouling alga *Enteromorpha*, Biofouling 18 (2002) 237–245.
[22] R.N. Wenzel, Resistance of solid surfaces to wetting by water, Ind. Eng. Chem. 28 (1936) 988–994.
[23] A.B.D. Cassie, S. Baxter, Wettability of porous surfaces, Faraday Soc. Trans. 40 (1944) 546–551.
[24] J.A. Finlay, M.E. Callow, L.K. Ista, G.P. Lopez, J.A. Callow, The influence of surface wettability on the adhesion strength of settled spores of the green alga *Enteromorpha* and the diatom *Amphora*, Integr. Comp. Biol. 42 (2002) 1116–1122.